Climate change hot-spots

F. Giorgi[1]

[1] A Regional Climate Change Index (RCCI), is developed based on regional mean precipitation change, mean surface air temperature change, and change in precipitation and temperature interannual variability. The RCCI is a comparative index designed to identify the most responsive regions to climate change, or Hot-Spots. The RCCI is calculated for 26 land regions from the latest set of climate change projections by 20 global climate models for the A1B, A2 and B1 IPCC emission scenarios. The Mediterranean and North Eastern European regions emerge as the primary Hot-Spots, followed by high latitude northern hemisphere regions and by Central America, the most prominent tropical Hot-Spot. The main African Hot-Spots are Southern Equatorial Africa and the Sahara. Eastern North America is the prominent Hot-Spot over the continental U.S. Different factors over different regions contribute to the magnitude of the RCCI, which is in fact greater than 0 for all regions. **Citation:** Giorgi, F. (2006), Climate change hot-spots, *Geophys. Res. Lett.*, *33*, L08707, doi:10.1029/2006GL025734.

1. Introduction

[2] The concept of climate change Hot-Spot can be approached from the viewpoint of vulnerability or from that of climate response. In the former case a Hot-Spot can be defined as a region for which potential climate change impacts on the environment or different activity sectors can be particularly pronounced. In the latter case, a Hot-Spot can be defined as a region whose climate is especially responsive to global change. In particular, the characterization of climate response-based Hot-Spots can provide key information to identify and investigate primary processes of regional climate change. From these premises, here the response approach is adopted to investigate climate change Hot-Spots based on results from a multi-model ensemble of climate change simulations performed by modeling groups from around the world as contributions to the Fourth Assessment Report of the Intergovernmental Panel on Climate Change (IPCC) (see the Program for Climate Model Diagnosis and Intercomparison, or PCMDI, http://www-pcmdi.llnl.gov).

[3] A Regional Climate Change Index (RCCI) is defined based on four variables: change in regional mean surface air temperature relative to the global average temperature change (or Regional Warming Amplification Factor, RWAF), change in mean regional precipitation (ΔP, % of present day value), change in regional surface air temperature interannual variability ($\Delta \sigma_T$, % of present day value), change in regional precipitation interannual variability ($\Delta \sigma_P$, % of present day value). In the definition of the RCCI it is important to include quantities other than the mean change because often mean changes are not the only important factors for determining impacts [e.g., *Mearns et al.*, 2001]. We thus also include interannual variability, which is critical for many activity sectors, such as agriculture or water management. The RCCI is calculated for the above mentioned set of global climate change simulations and is intercompared across regions to identify climate change Hot-Spots, that is regions with the largest values of RCCI.

[4] It is important to stress that, as will be seen, the RCCI is a comparative index, that is a small RCCI value does not imply a small absolute change, but only a small climate response compared to other regions.

2. Methodology

[5] Here "change" indicates the difference between the future 20-year climate period of 2080–2099 and a present day climate period minimally affected by greenhouse gas (GHG) forcing (1960–1979). As will be discussed later, the particular choice of these periods does not affect the basic conclusions of this paper. As a measure of temperature interannual variability we use the interannual standard deviation (σ_T) calculated for the selected 20-year periods. As a measure of precipitation variability we use the coefficient of variation (i.e., the standard deviation divided by the mean, here denoted as σ_P), which removes the dependency of the precipitation standard deviation on the mean. Both σ_T and σ_P are calculated after de-trending the data over the 20-year periods to obtain unbiased estimates of variability [*Räisänen*, 2002].

[6] The RCCI is calculated using wet season (WS) and dry season (DS) (Table 2) [as defined by *Giorgi and Bi*, 2005a, hereinafter referred to as GB05a] temperature and precipitation over 26 land regions of the world (see Figure 1) from 20 global model simulations (some including multiple realizations) of 20th and 21st climate under forcing from 3 IPCC emission scenarios, A1B, B1 and A2 [*Intergovernmental Panel on Climate Change*, 2000]. Note that these scenarios almost encompass the entire IPCC scenario range, the A2 being close to the high end of the range, the B1 close to the low end and the A1B lying toward the middle of the range. The model data are obtained from the PCMDI site and are interpolated onto a common 1 degree grid to facilitate intercomparison. More details on the data, models, simulations and definitions of regions are given by GB05a. The RCCI is defined as

$$RCCI = [n(\Delta P) + n(\Delta \sigma_P) + n(RWAF) + n(\Delta \sigma_T)]_{WS} + [n(\Delta P) + n(\Delta \sigma_P) + n(RWAF) + n(\Delta \sigma_T)]_{DS}$$

[1]Abdus Salam International Centre for Theoretical Physics, Trieste, Italy.
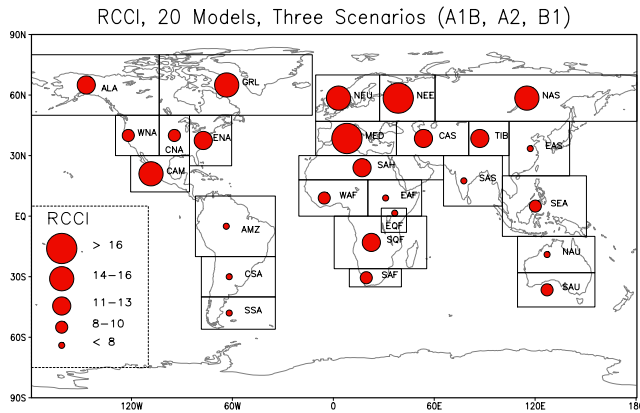
Figure 1. Regional Climate Change Index (RCCI) over 26 land regions of the World calculated from 20 coupled AOGCMs and 3 IPCC emission scenarios (A1B, A2, B1). The models used are BCCR-BCM2-0, CCMA-3-T47, CNRM-CM3, CSIRO-MK3, GFDL-CM2-0, GFDL-CM2-1, GISS-AOM, GISS-EH, GISS-ER, IAP-FGOALS, INMCM3, IPSL-CM4, MIROC3-2H, MIROC3-2M, MIUB-ECHO-G, MPI-ECHAM5, MRI-CGCM2, NCAR-CCSM3, NCAR-PCM1, UKMO-HADCM3. See also Table 1 of GB05a and http://www-pcmdi.llnl.gov.

where n is an integer varying from 0 to 4 as described in Table 1. Note that small changes below a certain threshold do not contribute to the index ($n = 0$) and that larger changes are weighted more heavily (i.e., the factor n doubles from each category to the next). As an illustrative example, ΔP is the change (2080–2099 minus 1960–1979) in average precipitation for a given region in Figure 1, (where only land points are included in the regional average, see GB05a) and is obtained via the following steps: 1) Calculate ΔP for each individual region and model simulation; 2) Average over the different realizations for the same model (if available); 3) Ensemble average over the different available models; 4) Average over the three scenarios (A1B, A2, B1). The same procedure is used to calculate the average regional values of RWAF, $\Delta \sigma_T$ and $\Delta \sigma_P$.

3. Results

[7] Figure 1 shows the RCCI for the different regions, while Table 2 presents the regional changes of relevant variables and the contributions of the different terms to the RCCI. The two most prominent Hot-Spots emerging from the RCCI analysis are the Mediterranean (MED) and North Eastern Europe (NEE) regions. The greatest contribution to the MED RCCI is given by a large decrease in mean precipitation and an increase in precipitation variability during the dry (warm) season. This summer drying signal, which makes the Mediterranean one of the most responsive regions to global change, has been consistently observed in different generations of model projections [*Giorgi et al.*, 2001; GB05a]. The main contributions to the NEE Hot-Spot are from a large increase in dry (cold) season precipitation, a large RWAF and an increase in precipitation interannual variability (Table 2). Note that, in agreement with previous studies [*Räisänen*, 2002; *Giorgi and Bi*, 2005b], Table 2 shows an increase in precipitation interannual variability

over most regions, an increase in temperature variability over warm climate regions and a decrease in temperature variability over mid- and high latitude cold climate regions.

[8] The main emerging tropical Hot-Spot is Central America (CAM), with primary contributions to the RCCI (Table 2) coming from a decrease in precipitation and an increase in precipitation variability (as measured by the coefficient of variation). Similarly to CAM, some high latitude cold climate regions (Northern Europe, NEU; Greenland, GRL; Northern Asia, NAS) also fall in the second highest Hot-Spot category. For GRL and NAS the greatest contribution is from a large RWAF and precipitation increase during winter, while for NEU the largest contribution is from changes in interannual variability (positive for precipitation and warm season temperature, negative for cold season temperature).

[9] In the third Hot-Spot category we find high latitude (Alaska, ALA), mid-latitude (Central Asia, CAS; Tibetan Plateau, TIB; Eastern North America, ENA), and sub-tropical (Sahara, SAH; South Equatorial Africa, SQF) regions. Table 2 shows that the main contributors to the RCCI vary from region to region. In particular, the main contribution to the index for the SQF region, which is the most pronounced Hot-Spot of sub-Saharan Africa, is associated with changes in interannual variability. By contrast, significant contributions to the RCCI for the ENA region come from all sources.

[10] An intermediate RCCI is found for the remaining two north American regions (Western North America, WNA; Central North America, CNA), two African regions (Western Africa, WAF; Southern Africa, SAF), Southern Australia (SAU), and South Eastern Asia (SEA). Finally the lowest RCCI values are found over a number of tropical and sub-tropical regions (Eastern Asia, EAS; Southern Asia, SAS; Northern Australia (NAU); Eastern Africa, EAF; Equatorial Africa (EQF); Amazon Basin (AMZ); Central South America, CSA; Southern South America, SSA). Although the total RCCI for these regions is not high, Table 2 shows that some individual contributions to the index may be large (e.g., a precipitation increase over the EQF region). In terms of the measures analyzed here, the South American regions appear to be generally less responsive to global change than other regions. However, we note that for all regions the RCCI is greater than 0, that is at least one of the RCCI components shows a change greater than the lowest threshold considered.

4. Discussion and Conclusions

[11] A few caveats need to be discussed to place Figure 1 into perspective. First, the thresholds used to define the different index categories and the values of the factor n in Equation 1 were subjectively chosen based on the distribution of the changes. However, the actual values of these

Table 1. Value of the Factor n in the Definition of the RCCI[a]

n	ΔP	$\Delta \sigma_P$	RWAF	$\Delta \sigma_T$
0	<5%	<5%	<1.1	<5%
1	5–10%	5–10%	1.1–1.3	5–10%
2	10–15%	10–20%	1.3–1.5	10–15%
4	>15%	>20%	>1.5	>15%

[a]See equation (1).

Table 2. Values of ΔP, $\Delta\sigma_P$, RWAF and $\Delta\sigma_T$ over the 26 Regions of Figure 1[a]

Region	Season	ΔP, %	$\Delta\sigma_P$, %	RWAF	$\Delta\sigma_T$, %	Season	ΔP, %	$\Delta\sigma_P$, %	RWAF	$\Delta\sigma_T$, %
NEU	WS (May–Oct)	0.85 (0)	17.39 (2)	1.13 (1)	15.09 (4)	DS (Nov–Apr)	14.40 (2)	6.69 (1)	1.43 (2)	−19.45 (4)
MED	WS (Oct–Mar)	−9.73 (1)	24.94 (4)	1.09 (0)	−3.43 (0)	DS (Apr–Sep)	−21.58 (4)	39.99 (4)	1.47 (2)	15.25 (4)
NEE	WS (May–Oct)	6.02 (1)	23.23 (4)	1.34 (2)	4.19 (0)	DS (Nov–Apr)	20.07 (4)	16.71 (2)	1.93 (4)	−12.40 (2)
NAS	WS (May–Oct)	11.40 (2)	14.69 (2)	1.39 (2)	3.39 (0)	DS (Nov–Apr)	27.27 (4)	9.41 (1)	1.96 (4)	5.28 (1)
CAS	WS (Nov–Apr)	−2.08 (0)	21.89 (4)	1.29 (1)	2.02 (0)	DS (May–Oct)	−9.26 (1)	16.13 (2)	1.55 (4)	4.31 (0)
TIB	WS (Apr–Sep)	7.94 (1)	3.15 (0)	1.42 (2)	3.00 (0)	DS (May–Oct)	15.93 (4)	12.62 (2)	1.54 (4)	3.61 (0)
EAS	WS (Apr–Sep)	8.20 (1)	9.81 (1)	1.20 (1)	3.03 (0)	DS (Oct–Mar)	6,87 (1)	1753 (2)	1.29 (1)	2.09 (0)
SAS	WS (May–Oct)	11.16 (2)	2.23 (0)	1.09 (0)	4.89 (0)	DS (Nov–Apr)	−2.28 (0)	8.82 (1)	1.31 (2)	9.99 (1)
SEA	WS (Apr–Sep)	6.84 (1)	12.24 (2)	0.95 (0)	−2.95 (0)	DS (Oct–Mar)	5.84 (1)	20.26 (4)	0.93 (0)	14.97 (2)
NAU	WS (Nov–Apr)	3.78 (0)	−1.07 (0)	1.20 (1)	8.61 (1)	DS (May–Oct)	−11.80 (2)	10.99 (2)	1.24 (1)	3.96 (0)
SAU	WS (May–Oct)	−13.06 (2)	20.52 (4)	1.00 (0)	14.81 (2)	DS (Nov–Apr)	2.90 (0)	5.58 (1)	1.09 (0)	8.08 (1)
SAH	WS (Nov–Apr)	−17.11 (4)	19.71 (2)	1.28 (1)	7.36 (1)	DS (May–Oct)	−2.34 (0)	2.80 (0)	1.48 (2)	5.20 (1)
WAF	WS (May–Oct)	1.01 (0)	6.11 (1)	1.23 (1)	6.88 (1)	DS (Nov–Apr)	0.52 (0)	11.87 (2)	1.25 (1)	12.56 (2)
EAF	WS (May–Oct)	4.45 (0)	2.01 (0)	1.22 (1)	10.89 (2)	DS (Nov–Apr)	10.25 (2)	1.92 (0)	1.21 (1)	1.34 (0)
EQF	WS (Feb–Jul)	12.00 (2)	−3.85 (0)	1.11 (1)	7.26 (1)	DS (Aug–Jan)	12.64 (2)	−7.41 (1)	1.09 (0)	2.69 (0)
SQF	WS (Nov–Apr)	1.80 (0)	20.74 (4)	1.18 (1)	15.99 (4)	DS (May–Oct)	−7.18 (1)	4.63 (0)	1.28 (1)	12.17 (2)
SAF	WS (Oct–Mar)	−0.67 (0)	−4.31 (0)	1.21 (1)	−6.67 (1)	DS (Apr–Sep)	−11.61 (2)	14.32 (2)	1.24 (1)	5.04 (1)
ALA	WS (Jun–Nov)	13.47 (2)	3.28 (0)	1.35 (2)	−3.86 (0)	DS (Dec–May)	18.72 (4)	−2.12 (0)	1.80 (4)	−5.51 (1)
GRL	WS (Jun–Nov)	13.58 (2)	1.67 (0)	1.45 (2)	−14.96 (2)	DS (Dec–May)	20.48 (4)	9.24 (1)	1.85 (4)	−5.37 (1)
WNA	WS (Oct–Mar)	5.48 (1)	7.09 (1)	1.27 (1)	−6.42 (1)	DS (Apr–Sep)	−6.71 (1)	8.63 (1)	1.49 (2)	7.10 (1)
CNA	WS (Apr–Sep)	−1.39 (0)	18.80 (2)	1.49 (2)	10.37 (2)	DS (Oct–Mar)	4.39 (0)	6.68 (1)	1.37 (2)	−8.98 (1)
ENA	WS (Apr–Sep)	4.02 (0)	19.18 (2)	1.34 (2)	8.58 (1)	DS (Oct–Mar)	11.38 (2)	11.99 (2)	1.41 (2)	−12.18 (2)
CAM	WS (May–Oct)	−9.44 (1)	15.20 (2)	1.24 (1)	6.65 (1)	DS (Nov–Apr)	−17.34 (4)	26.67 (4)	1.28 (1)	7.63 (1)
AMZ	WS (Nov–Apr)	4.02 (0)	1.81 (0)	1.16 (1)	3.73 (0)	DS (May–Oct)	−4.49 (0)	16.61 (2)	1.32 (2)	9.39 (1)
CSA	WS (Oct–Mar)	3.90 (0)	8.06 (1)	1.11 (1)	4.44 (0)	DS (Apr–Sep)	−2.52 (0)	17.67 (2)	1.04 (0)	5.74 (1)
SSA	WS (Apr–Sep)	−0.33 (0)	8.03 (1)	0.71 (0)	−12.56 (2)	DS (Oct–Mar)	−10.02 (2)	9.70 (1)	0.80 (0)	4.82 (0)

[a]See text for further information on values. WS is the wet season and DS is the dry season. The changes are calculated for the period 2080–2099 compared to 1960–1979 and are averaged over the A1B, A2, and B1 scenarios. The corresponding value of n in equation (1) is shown in parentheses.

thresholds are not important, as the main objective of the RCCI analysis is to compare regions with each other and not to provide an absolute measure of change. Changes in these thresholds might lead to variations in the RCCI regional values, but would not modify the overall picture given by Figure 1. As already mentioned, the RCCI is a comparative index and does not reflect absolute changes.

[12] Second, for the calculations shown here we used the last 20 year period of the 21st century in order to maximize the change signal. Also, the results were averaged across the three scenarios considered. However, with proper scaling, the same general picture was found for individual scenarios and earlier 20 year periods of the 21st century. Previous studies [*Mitchell*, 2003; *Giorgi*, 2005] have shown that regional temperature and (to a lesser extent) precipitation changes scale relatively well with the GHG forcing, in particular for relatively large signals. Therefore, the basic results described here, properly scaled, apply more generally.

[13] Third, the RCCI is only based on mean changes and changes in interannual variability. Measures of changes in extremes might also be added to make the index more general. A few test calculations showed that changes in the occurrence of extreme seasons followed closely the changes in interannual variability, so that the latter can be also considered as a measure of change in seasonal scale extremes. In addition, if the distribution of events does not change or widens in future climate conditions, a shift in the mean would also imply a corresponding shift in extremes.

[14] Finally, all the variables and statistical moments were equally weighted in the calculation of the RCCI. However, it would be easily possible to weight variables and models based, for example, on performance skill in the calculation of the RCCI (e.g., GB05a).

[15] With these cavetas in mind, the analysis presented here identifies the Mediterranean and Northeastern Europe regions as the most prominent climate response Hot-Spots, followed by high latitude northern hemisphere regions and Central America. The latter appears to be the primary Hot-Spot in the tropics, immediately followed by Southern Equatorial Africa and Southeast Asia. Other prominent mid-latitude Hot-Spot regions are Eastern North America and Central Asia. The occurrence of a certain Hot-Spot might be due to local feedbacks (e.g., snow-sea ice albedo feedback or the soil moisture-precipitation feedback) or to changes in circulations and modes of natural variability [e.g., *Corti et al.*, 1999; *Terray et al.*, 2004; *Meehl and Tebaldi*, 2004; *Collins et al.*, 2005; *Coppola et al.*, 2005; *Meehl et al.*, 2005; *Rowell and Jones*, 2006] so that each Hot-Spot needs to be analysed individually to identify key response mechanisms.

References

Collins, M., and The CMIP Modelling Groups (2005), El Niño- or La Niña-like climate change?, *Clim. Dyn.*, 24, 89–104.

Coppola, E., F. Kucharski, F. Giorgi, and F. Molteni (2005), Bimodality of the North Atlantic Oscillation in simulations with greenhouse gas forcing, *Geophys. Res. Lett.*, 32, L23709, doi:10.1029/2005GL024080.

Corti, S., F. Molteni, and T. N. Palmer (1999), Signature of recent climate change in frequencies of natural atmospheric circulation regimes, *Nature*, 398, 799–802.

Giorgi, F. (2005), Interdecadal variability of regional climate change: Implications for the development of regional climate change scenarios, *Meteorol. Atmos. Phys.*, *89*, 1–15.

Giorgi, F., and X. Bi (2005a), Updated regional precipitation and temperature changes for the 21st century from ensembles of recent AOGCM simulations, *Geophys. Res. Lett.*, *32*, L21715, doi:10.1029/2005GL024288.

Giorgi, F., and X. Bi (2005b), Regional changes in surface climate interannual variability for the 21st century from ensembles of global model simulations, *Geophys. Res. Lett.*, *32*, L13701, doi:10.1029/2005GL023002.

Giorgi, F., P. W. Whetton, R. G. Jones, J. H. Christensen, L. O. Mearns, B. Hewitson, H. vonStorch, R. Francisco, and C. Jack (2001), Emerging patterns of simulated regional climatic changes for the 21st century due to anthropogenic forcings, *Geophys. Res. Lett.*, *28*, 3317–3320.

Intergovernmental Panel on Climate Change (2000), *Special Report on Emissions Scenarios*, edited by N. Nakicenovic et al., 599 pp., Cambridge University Press, New York.

Mearns, L. O., et al. (2001), Climate scenario development, in *Climate Change 2001: The Scientific Basis: Contribution of Working Group I to the Third Assessment Report of the Intergovernmental Panel on Climate Change*, edited by J. T. Houghton et al., pp. 739–768, Cambridge University Press, New York.

Meehl, G. A., and C. Tebaldi (2004), More intense, more frequent and longer lasting heat waves in the 21st century, *Science*, *305*, 994–997.

Meehl, G. A., J. M. Arblaster, and C. Tebaldi (2005), Understanding future patterns of increased precipitation intensity in climate model simulations, *Geophys. Res. Lett.*, *32*, L18719, doi:10.1029/2005GL023680.

Mitchell, T. D. (2003), Pattern Scaling: An examination of the accuracy of the technique for describing future climates, *Clim. Change*, *60*, 217–242.

Räisänen, J. (2002), CO_2-induced changes in interannual temperature and precipitation variability in 19 CMIP2 experiments, *J. Clim.*, *15*, 2395–2411.

Rowell, D. P., and R. G. Jones (2006), The causes and uncertainty of future summer drying over Europe, *Clim. Dyn.*, in press.

Terray, L., M. E. Demory, M. Deque, G. de Coetlogon, and E. Maisonnave (2004), Simulation of late-twenty-first-century changes in wintertime atmospheric circulation over Europe due to anthropogenic causes, *J. Clim.*, *17*, 4630–4635.

————————————

F. Giorgi, Abdus Salam International Centre for Theoretical Physics, Strada Costiera 11, I-34014 Trieste, Italy. (giorgi@ictp.it)